Tungsten (2023) 5:598–606
https://doi.org/10.1007/s42864-023-00217-1

Tungsten
www.springer.com/42864

ORIGINAL PAPER

Tungsten doping $La_{0.6}Ca_{0.4}Fe_{0.8}Ni_{0.2}O_{3-\delta}$ as electrode for highly efficient and stable symmetric solid oxide cells

Xin-Yi Jiao[1] · Ao-Yan Geng[1] · Yi-Yang Xue[1] · Xing-Bao Wang[2] · Fang-Jun Jin[1] · Yi-Han Ling[1] · Yun-Feng Tian[1]

Received: 8 December 2022 / Revised: 3 January 2023 / Accepted: 4 January 2023 / Published online: 13 April 2023

Abstract
Perovskite oxide $La_{0.6}Ca_{0.4}Fe_{0.8}Ni_{0.2}O_{3-\delta}$ (LCFN) has been used in symmetric solid oxide cells (SSOCs) to obtain good electrochemical performance in both fuel cells (SOFCs) and electrolysis cells (SOECs) modes. However, its structural stability still faces challenges and the electrocatalytic activity also needs to be further improved. Herein, tungsten-doped $La_{0.6}Ca_{0.4}Fe_{0.7}Ni_{0.2}W_{0.1}O_{3-\delta}$ (LCFNW) perovskite oxide material was synthesized which exhibits good structural stability under H_2 and superior electrochemical performance as an electrode for SSOCs. In SOFCs mode, the cell achieved the maximum power density of 0.58 $W{\cdot}cm^{-2}$ with wet H_2 as fuel at 850 °C. In SOECs mode, the current density can reach 1.81 $A{\cdot}cm^{-2}$ for pure CO_2 electrolysis at 2 V. Moreover, the SSOCs exhibits outstanding long-term stability in both SOFCs and SOECs modes, proving that doping W in perovskite oxide is an effective strategy to enhance the catalytic activity and stability of the electrode. The LCFNW material developed in this work shows promising prospect as an electrode candidate for SSOCs.

Keywords Symmetric solid oxide cells · Perovskite oxide · $La_{0.6}Ca_{0.4}Fe_{0.7}Ni_{0.2}W_{0.1}O_{3-\delta}$ · CO_2 electrolysis · Stability

1 Introduction

Solid oxide cells (SOCs) can efficiently convert chemical energy into electricity in solid oxide fuel cells (SOFCs) mode, which has the special advantages of flexible fuel, high energy conversion efficiency, high power density and low environmental pollution [1, 2]. In addition, it can also operate reversely as solid oxide electrolysis cells (SOECs), using renewable energy to electrolyze H_2O to produce H_2 [3], electrolyze CO_2 to reduce carbon emissions [4], and co-electrolyze H_2O–CO_2 to produce syngas for subsequent chemical production [5]. A traditional SOCs is composed of dense electrolyte, porous perovskite oxide air electrode and porous metal cermet fuel electrode. However, there is a high risk of carbon deposition and sulfur poisoning for Ni-based cermet electrode [6]. Moreover, Ni-based cermet electrodes also face the problem of redox instability, metal agglomeration and growth [7], etc. In addition, traditional perovskite oxide cathodes such as $La_{0.8}Sr_{0.2}MnO_{3-\delta}$ (LSM) and $La_{0.6}Sr_{0.4}Co_{0.2}Fe_{0.8}O_{3-\delta}$ (LSCF) still have problems such as poor activity and stability [8, 9]. Therefore, it is urgent to develop high electrocatalytic activity and stable oxide materials as SOCs air electrode and fuel electrode. If the fuel electrode and air electrode use the same material, named symmetric solid oxide cells (SSOCs), it can greatly reduce the manufacturing cost and improve the compatibility between electrolyte and electrode. Moreover, this unique symmetric structure can be flexibly switched between SOFCs mode and SOECs mode, which have attracted great attention [10–12].

As shown in Fig. 1, the electrode needs to meet high catalytic activity requirements towards hydrogen oxide reaction (HOR) and oxygen reduction reaction (ORR) in SOFCs mode, and carbon dioxide reduction reaction (CO_2RR) and oxygen evolution reaction (OER) in SOECs mode, all of which need to be implemented on the same material, so the electrode materials are the key to the development of symmetric cells. Badding et al. [13] first proposed the concept of symmetrical cell in 2003. Since then, many new

✉ Yi-Han Ling
lyhyy@cumt.edu.cn

✉ Yun-Feng Tian
yunfengup@cumt.edu.cn

[1] School of Materials Science and Physics, China University of Mining and Technology, Xuzhou 221116, China

[2] State Key Laboratory of Clean and Efficient Coal Utilization, Taiyuan University of Technology, Taiyuan 030024, China

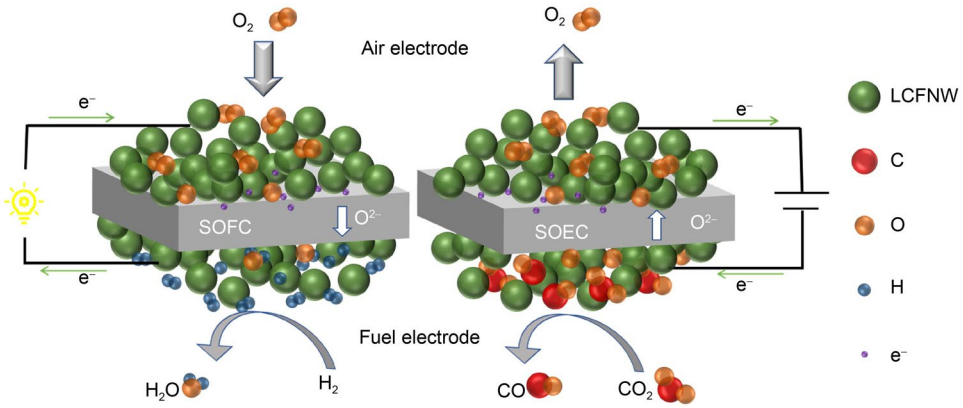

Fig. 1 Schematic diagram of the reaction process of the symmetric solid oxide cells (SSOCs)

materials have been developed for SSOCs. For example, Fan et al. [14] used nanoporous $Sm_{0.95}Ce_{0.05}FeO_{3-\delta}$ as electrode, the maximum power density of 130 mW·cm^{-2} can be achieved in pure H_2 at 800 °C. Ma et al. [15] used Ni doped $La_{0.6}Sr_{0.4}FeO_{3-\delta}$ (LSFN) as electrode material, and prepared symmetric cell by the impregnation method. Using C_3H_8 and CH_4 as fuel, it was found that the electrode showed good stability in long-term test and had good catalytic activity for hydrocarbon fuel oxidation. Rath et al. [16] developed a novel double perovskite electrode $Sr_2ScTi_{1-x}Mo_xO_6$, which confirmed that the electrode exhibited excellent catalytic activity for the oxidation of hydrogen and methane as well as the oxygen reduction reaction. The maximum power density of $La_{0.8}Sr_{0.2}Ca_{0.8}Mg_{0.2}O_{3-\delta}$ (LSGM) electrolyte-supported $Sr_{0.8}Ce_{0.2}FeO_3$ symmetric fuel cell reaches 482 mW·cm^{-2} at 800 ℃, and it also shows good structural stability [17]. Although the development of symmetric cells with these materials have seen significant progress in recent years, their electrochemical performance is still inferior to conventional cells. Therefore, it is imperative to develop novel SSOCs electrode materials with high catalytic activity and stability.

$LaFeO_3$ perovskite material has good structural stability and electrocatalytic activity. The well-known LSCF material is derived from it [18]. Although LSCF has achieved good electrochemical performance as a SOCs electrode, its stability still faces challenges, mainly because Sr easily segregates at high temperature and current polarization, and easily reacts with CO_2 to form $SrCO_3$ which leads to the degradation of the catalytic performance of the electrode [19]. In addition, the high thermal expansion coefficient of LSCF leads to the weak binding of the electrode–electrolyte interface [20]. In our previous work [21, 22], $La_{0.6}Ca_{0.4}Fe_{0.8}Ni_{0.2}O_{3-\delta}$ (LCFN) was synthesized by replacing Sr and Co with Ca and Ni, respectively, to obtain higher electrical conductivity, lower thermal expansion coefficient, and higher electrochemical performance. However, whether it is LSCF or LCFN, its structural stability under H_2 is insufficient. Therefore, it is urgent to improve its structural stability.

Many studies have shown that high-valence metal such as Ti, Nb, V, Sc doping perovskite oxides can effectively improve the electrocatalytic activity and structural stability of the material [23–27]. Herein, W was selected as the B-site doping element and the prepared $La_{0.6}Ca_{0.4}Fe_{0.7}Ni_{0.2}W_{0.1}O_{3-\delta}$ (LCFNW) showed excellent structural stability, high electrical conductivity, and low thermal expansion coefficient. Good electrochemical performance has also been achieved as an electrode for SSOCs. In SOFCs mode, the cell achieved the maximum power density of 0.58 W·cm^{-2} with wet H_2 as fuel at 850 °C. In SOECs mode, the current density can reach 1.81 A·cm^{-2} for pure CO_2 electrolysis at 2 V. The cell also shows good stability in both SOFCs and SOECs modes.

2 Experimental

2.1 Synthesis of powder

The raw material $La(NO_3)_3$, $Ca(NO_3)_2$, $Fe(NO_3)_3$, $Ni(NO_3)_2$ and $H_{40}N_{10}O_{41}W_{12}{\cdot}xH_2O$ was weighed according to the stoichiometric ratio of LCFNW and were dissolved in deionized water. Then, citric acid (CA) and ethylenediaminetetraacetic acid (EDTA) were added according to the molar ratio of metal ions: CA: EDTA of 1:1:1.5. Ammonia solution was then added with continuous stirring until the pH value of the solution was 8. The gel was formed after the water evaporated and then dried at 240 °C to obtain the precursor. Finally, the precursor was fully ground in a mortar and calcined at 1200 °C in a muffle furnace to obtain the required electrode powders. LCFN powders was also prepared by the same method.

2.2 Preparation of cells

$Y_{0.08}Zr_{0.92}O_{2-\delta}$ (YSZ) electrolytes with 12 mm in diameter and 0.3 mm in thickness were prepared by tape casting method. Then it was placed in a furnace and

sintered at 1500 °C for 10 h to obtain the dense electrolyte. $Gd_{0.1}Ce_{0.9}O_{2-\delta}$ (GDC) was used as a buffer layer to prevent phase reactions between electrode and YSZ. The GDC slurry was coated on both sides of the YSZ electrolyte and then calcined at 1300 °C for 5 h. LCFNW electrode slurry was prepared by mixing LCFNW powder with the binder at a mass ratio of 6:4. The prepared LCFNW slurry was coated on both sides of the electrolyte and calcined in air at 1000 °C for 2 h. For LCFNW-GDC composite electrode. The mass ratio of LCFNW to GDC is 6:4. Silver paste was coated on the surface of the cell as the current collector.

2.3 Characterization and cell measurement

X-ray diffraction (XRD Shimadzu XRD-7000S, voltage: 40 kV, current: 30 mA, angle range 20°–80°, scanning speed: $10°\cdot min^{-1}$) was used to analyze the phase structure of the material. The microstructure of the samples was analyzed by Scanning Electron Microscope (SEM Sirion 200). The LCFNW electrode powder was pressed into 24 mm × 6 mm × 2 mm bar sample by dry pressing method and sintered at 1250 °C for 5 h for subsequent thermal expansion coefficient and conductivity test. The conductivity of LCFNW bar sample was measured by Agilent B2901A Precision Source/Measurement unit using a four-probe method. The thermal expansion coefficient of the material was tested by a thermal dilatometer (NETZSCH DIL402C, Germany). The electrochemical performance of the cell was tested by Zahner IM6 Electrochemical Workstation. The SOFCs performance with wet H_2 as fuel and the SOECs performance of electrolytic pure CO_2 were explored through AC impedance spectroscopy, current–voltage curve test and stability test at different temperatures.

3 Results and discussion

3.1 Physicochemical properties

Figure 2a shows the XRD patterns of LCFN and LCFNW powders synthesized by sol–gel method. It can be seen that both samples have a good perovskite structure according to PDF card#82-1946. However, some minor unknown phase exists in LCFNW. In fact, these unknown phase does not affect the catalytic performance of the electrode material, which will be investigated later. It is worth mentioning that the crystal structure of LCFNW after treated in H_2 at 800 °C for 5 h (named R-LCFNW) remains stable. However, the structure of LCFN was destroyed under the same reduction conditions. In addition, the peak at about 44° represents the exsolution of Fe–Ni alloy, indicating that the nano-alloy particles are in situ exsolved from the R-LCFNW. Moreover, when LCFNW and GDC mixed with a mass ratio of 1:1 was calcined at 1000 °C for 5 h, no impurity peaks appeared as shown in Fig. 2b, which proved that LCFNW and GDC had good chemical compatibility. Overall, W doping can effectively improve the stability of the LCFN crystal structure.

Figure 3a shows the conductivity test results of LCFNW in air. It can be seen that the conductivity increases with the increase of temperature, showing the semiconductor conductive properties. The conductivity reaches the maximum of 15 $S\cdot cm^{-1}$ at about 800 °C. With the increase of temperature, the small polaron (Fe^{4+}, Fe^{3+}, Ni^{2+}, W^{6+})–O^{2-}–(Fe^{2+}, Ni^{+}, W^{4+}) activity induced by thermal excitation increases, resulting in the improvement of conductivity. When the temperature reaches a certain level (> 800 °C), some Fe^{3+}, Ni^{2+}, W^{6+} metal cations will undergo thermal reduction reaction, and transform into low-valence cations, resulting in the formation of oxygen vacancies. This will

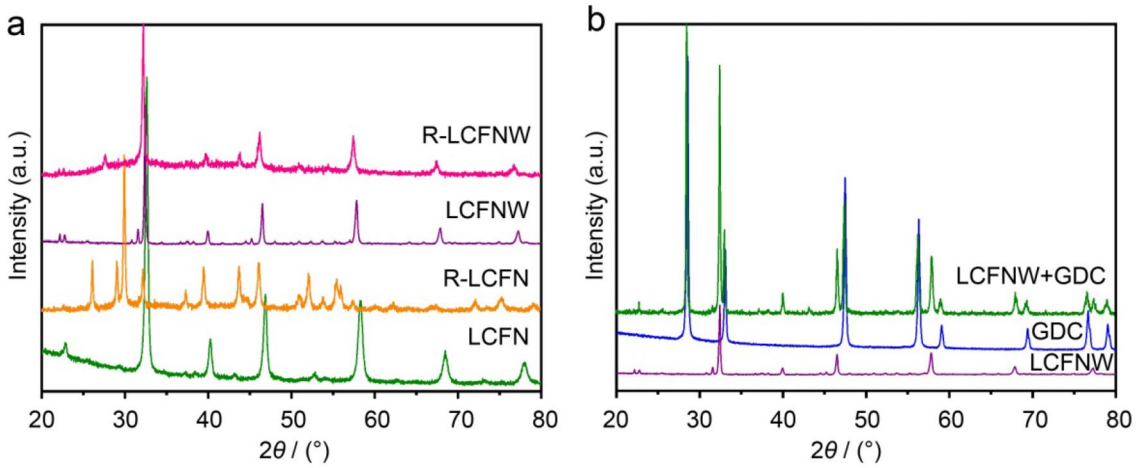

Fig. 2 **a** XRD patterns of LCFN and LCFNW in air and hydrogen. **b** Chemical compatibility of LCFNW and GDC sintered at 1000 °C for 5 h

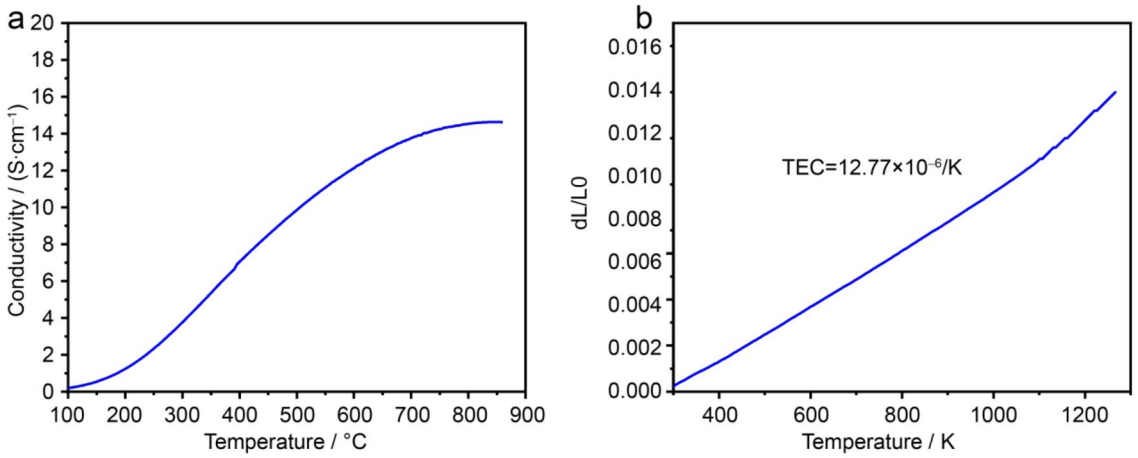

Fig. 3 **a** The conductivity and **b** thermal expansion coefficient of LCFNW in air

reduce the carrier concentration and eventually leads to the decrease of conductivity [28]. Figure 3b is the measured thermal expansion curve of LCFNW. After calculation, the average thermal expansion coefficient (TEC) is 12.77×10^{-6} K^{-1}, which is very close to the thermal expansion coefficient of GDC (12×10^{-6} K^{-1}) [29]. Moreover, the TEC value is also much lower than that of Co-based electrode materials such as $SrCo_{0.9}Nb_{0.1}O_{3-\delta}$ (24.2×10^{-6} K^{-1}) [30], $La_{0.3}Sr_{0.7}Ti_{0.7}Co_{0.3}O_{3-\delta}$ (20.7×10^{-6} K^{-1}) [31], $Ba_{0.5}Sr_{0.5}Co_{0.8}Fe_{0.2}O_{3-\delta}$ (21.6×10^{-6} K^{-1}) [32]. Having a TEC value close to GDC can make the electrode and GDC barrier layer well-adhered and result in decent thermal mechanical compatibility, which is beneficial to the long-term stability of the cell. It is worth noting that the TEC of LCFNW increases more significantly over 800 °C. Because the valence of metal cations changes at high temperature, resulting in the escape of lattice oxygen and the formation of oxygen vacancies, it thereby leads to a change in the slope of the thermal expansion curve. This is also consistent with the previous turning point for conductivity results.

3.2 Electrochemical performance in SOFCs mode

Figure 4a shows the I–V–P curves and b Electrochemical impedance spectrum (EIS) of the symmetric cell with pure LCFNW electrode at different temperatures when using wet H_2 as fuel. The open circuit voltage (OCV) is basically consistent with the theoretical OCV calculated by the Nernst equation, indicating the good tightness of YSZ electrolyte and well sealing of the cell. Figure 4a shows the maximum power density (MPD) of the symmetric cell at 750, 800 and 850 °C, which is 0.110, 0.211, 0.327 $W\cdot cm^{-2}$, respectively. Moreover, the I–V–P curve did not show noticeable concentration polarization phenomenon. For EIS as shown in Fig. 4b, the ohmic resistance (R_s) of symmetric cell at 750, 800 and 850 °C is 1.65, 0.86 and 0.58 $\Omega\cdot cm^2$; and the polarization resistance (R_p) are 1.06, 0.46 and 0.32 $\Omega\cdot cm^2$, respectively. It can be seen that R_s and R_p decrease greatly with the increase of temperature. Increasing the temperature is beneficial to the ion transport of the electrolyte and the improvement of the electrochemical activity.

In order to further enhance the electrocatalytic activity of the electrode, LCFNW-GDC composite electrode was prepared and the I–V–P curves of LCFNW-GDC symmetric cell at different temperatures were shown in Fig. 4c. The MPD of the symmetrical cell at 700, 750, 800 and 850 °C is 0.11, 0.25, 0.38 and 0.58 $W\cdot cm^{-2}$, respectively. Compared with pure LCFNW electrodes, the power density has been significantly improved. Moreover, compared with previous studies as listed in Table 1, The performance is also good, suggesting that the W doping LCFN can reinforce the electrocatalytic performance of electrode materials. Figure 4d shows the EIS of LCFNW-GDC symmetric cell at different temperatures. The R_s and R_p of the cell at 700, 750, 800 and 850 °C is 1.07, 0.56, 0.38, 0.26 $\Omega\cdot cm^2$ and 0.77, 0.36, 0.25 and 0.18 $\Omega\cdot cm^2$, respectively. And the R_p is also lower than pure LCFNW electrode and other electrodes such as the $SmBaMn_2O_{5+\delta}$ (1.23 $\Omega\cdot cm^2$) [40], $Sr_2ScTi_{0.9}Mo_{0.1}O_6$ (0.29 $\Omega\cdot cm^2$) at 800 °C [16]. In brief, higher MPD and lower R_p demonstrate the good HOR and ORR catalytic activity of LCFNW.

3.3 Electrochemical performance in SOECs mode

Figure 5a is the I–V curves of LCFNW-GDC symmetric cell for pure CO_2 electrolysis at different temperatures. It can be seen that the current density gradually rises with the increase of applied voltage. When the electrolysis voltage is greater than 1 V, the electrolysis current density increases rapidly with the increase of voltage, indicating

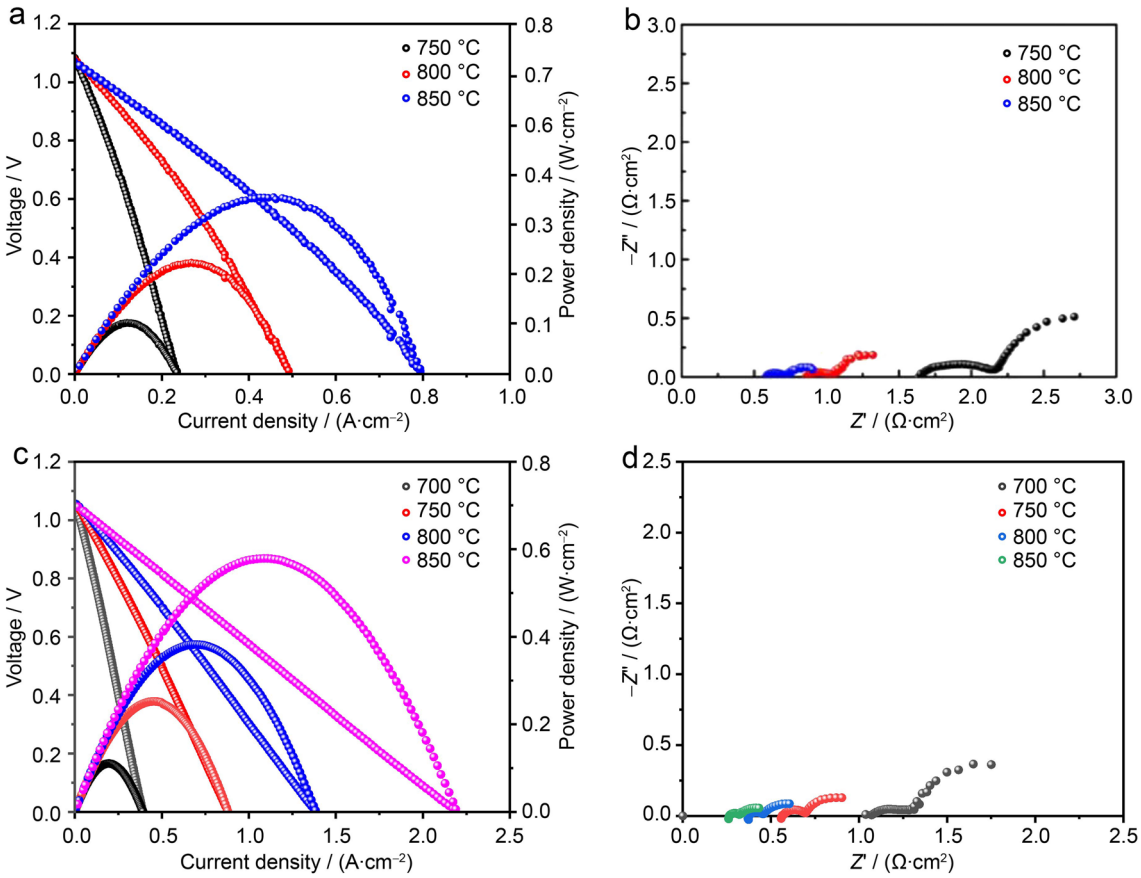

Fig. 4 **a** The I–V–P curve and **b** EIS of symmetric cell based pure LCFNW electrode, **c** the I–V–P curve and **d** EIS of symmetric cell based LCFNW-GDC composite electrode at different temperatures in SOFCs mode

Table 1 The summarized performance of SOFCs with different electrodes

Electrode	Electrolyte	Test conditions	Power density ($W·cm^{-2}$)	R_p ($Ω·cm^2$)	References
$La_{0.6}Ca_{0.4}Fe_{0.7}Ni_{0.2}W_{0.1}O_{3-\delta}$-GDC (this work)	YSZ	800@H_2	0.38	0.25	
		850@H_2	0.58	0.18	
$PrBaMn_2O_{5+\delta}$-YSZ	YSZ	800@H_2	0.253	0.26	[33]
$La_{0.75}Sr_{0.25}Cr_{0.5}Mn_{0.5}O_{3-\delta}$	YSZ	900@H_2	0.3	0.3	[34]
$Sr_2Fe_{1.5}Mo_{0.5}O_{6-\delta}$-GDC	YSZ	750@H_2	0.191	0.53	[35]
$La_{0.8}Sr_{0.2}FeO_{3-\delta}$-GDC	YSZ	800@H_2	0.387	0.58	[36]
$La_{0.75}Sr_{0.25}Cr_{0.5}Mn_{0.5}O_{3-\delta}$-YSZ	YSZ	950@H_2	0.546	0.29	[37]
$La_{0.8}Sr_{0.2}MnO_{3-\delta}$-GDC	YSZ	800@H_2	0.158	5.19	[38]
$CaFe_{0.4}Ti_{0.6}O_{3-\delta}$	YSZ	800@H_2	0.058	1	[39]

the electrolysis process of CO_2 begins. With the increase of temperature, the maximum current densities of 0.88, 1.34 and 1.8 $A·cm^{-2}$ at 750, 800 and 850 °C can be achieved at 2.0 V, respectively. Figure 5b is EIS of LCFNW-GDC cell at different temperatures. It is found that the R_s and R_p of the cell decrease with the increase of temperature. At 750, 800 and 850 °C, the R_s and R_p of the cell were 1.60, 1.26, 1.11 $Ω·cm^2$ and 3.40, 1.93, 1.27 $Ω·cm^2$, respectively. The electrolysis performance is also better than other symmetric cells such as $La_{0.3}Sr_{0.7}Fe_{0.7}Ti_{0.3}O_3$ (0.521 $A·cm^{-2}$) [41], $La_{0.3}Sr_{0.7}Fe_{0.7}Cr_{0.3}O_{3-\delta}$ (0.41$A·cm^{-2}$@1.5 V) [42], $La_{0.6}Sr_{0.4}Fe_{0.9}Mn_{0.1}O_{3-\delta}$ (1.107 $A·cm^{-2}$@2.0 V) [43] at 800 °C, etc. In short, the LCFNW electrode has good CO_2RR catalytic activity and OER catalytic activity.

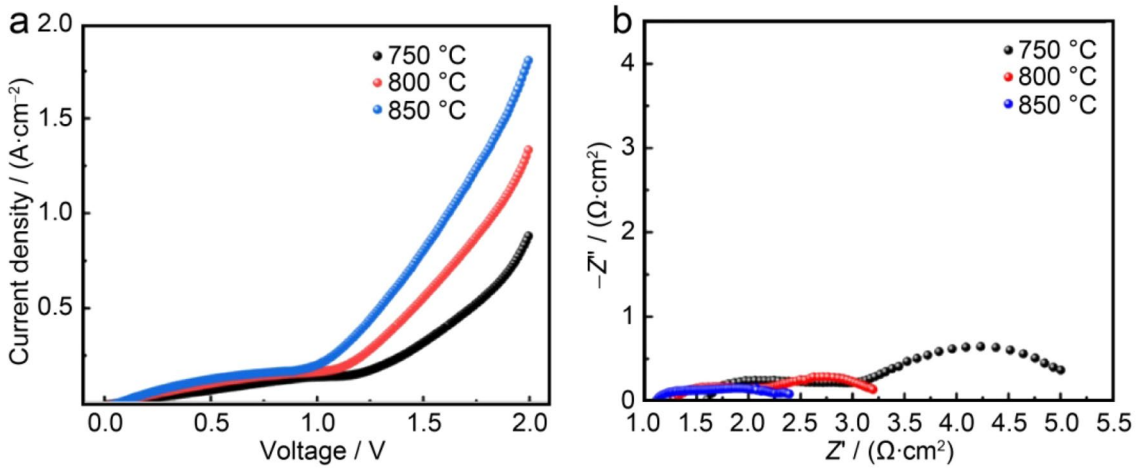

Fig. 5 **a** I–V curves and **b** EIS of LCFNW-GDC symmetric cell for pure CO_2 electrolysis at different temperatures

3.4 Stability test in SOFCs and SOECs mode

To test the stability of the LCFNW-GDC symmetric cell in SOFCs mode, both the short-term and long-term durability tests at 0.7 V were measured as shown in Fig. 6a, b. It can be seen the performance of the cell keeps all stable in short-term and long-term tests at 750 °C and 700 °C. Moreover, the EIS of the cell before and after the stability test was measured as shown in Fig. 6c. It can be seen that the R_s and R_p of the cell are slightly reduced after stability test. The reason may be due to the exsolution of a large number of Fe–Ni alloy nanoparticles on the surface of LCFNW under high temperature and reducing atmosphere, which is beneficial to the electrocatalytic and conductivity of LCFNW electrode. It is also confirmed by the XRD results mentioned before.

Figure 7a is the EIS of the symmetric cell measured at 1.4 V for pure CO_2 electrolysis at different temperatures. At 750, 800 and 850 °C, the R_s and R_p of the cell were 1.32, 0.87, 0.59 Ω·cm^2 and 2.57, 1.62, 0.50 Ω·cm^2, respectively. It can be found that the higher the temperature, the smaller the R_s and R_p. At the same time, the durability tests under different voltages were also carried out as shown in Fig. 7b. It can be seen that the cell performance is relatively stable at low voltage, but with the increase of the electrolysis voltage, the cell performance is slightly attenuated, the reason may be that the lack of CO_2 in the cathode gas and the slow oxygen evolution reaction (OER) of the cell at high voltage cause the cell performance degradation [44]. Therefore, LCFNW symmetric cell is suitable for operation under 1.4 V. Figure 7c shows the stability test of LCFNW-GDC symmetric cell for pure CO_2 electrolysis at 750 °C for 40 h at 1.4 V. The current density gradually decreased in the first 10 h, then it remained steady at around 100 mA·cm^{-2}. Overall, the LCFNW electrode has good stability for pure CO_2 electrolysis.

The microstructure of the symmetric cell after the stability test is shown in Fig. 8. As can be seen from Fig. 8a, c, both the cathode and anode were tightly bound to the GDC layer. There is still existing a good electrode/electrolyte interface with no signs of cracking and delamination after SOFCs and SOECs stability test. The thickness of the

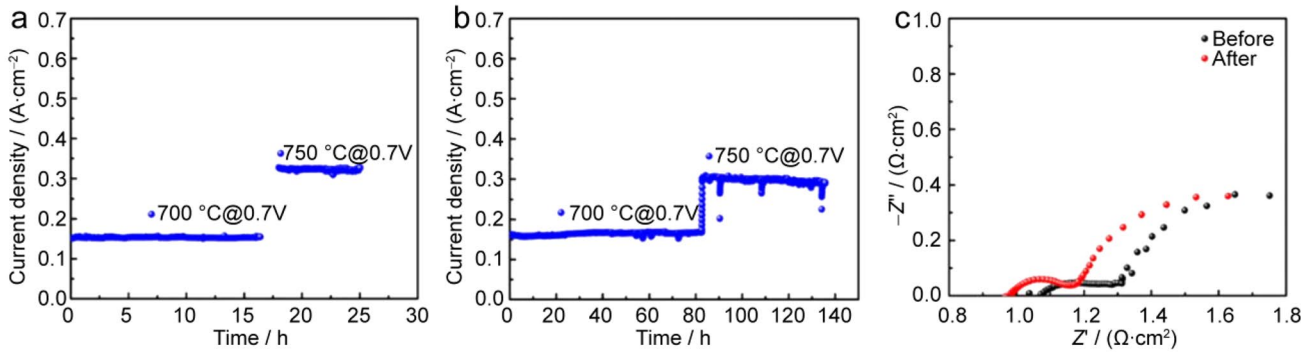

Fig. 6 **a** Short-term durability test, **b** long-term durability test at different conditions and **c** the EIS of the cell before and after stability test in SOFCs mode

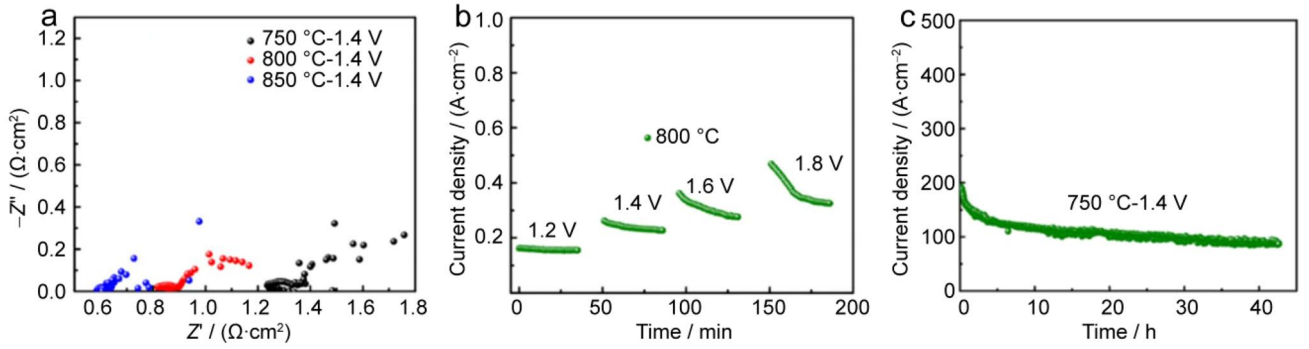

Fig. 7 **a** EIS of LCFNW-GDC symmetric cell for pure CO_2 electrolysis at different temperatures at 1.4 V, **b** short-term durability tests at different voltages and **c** long-term durability tests

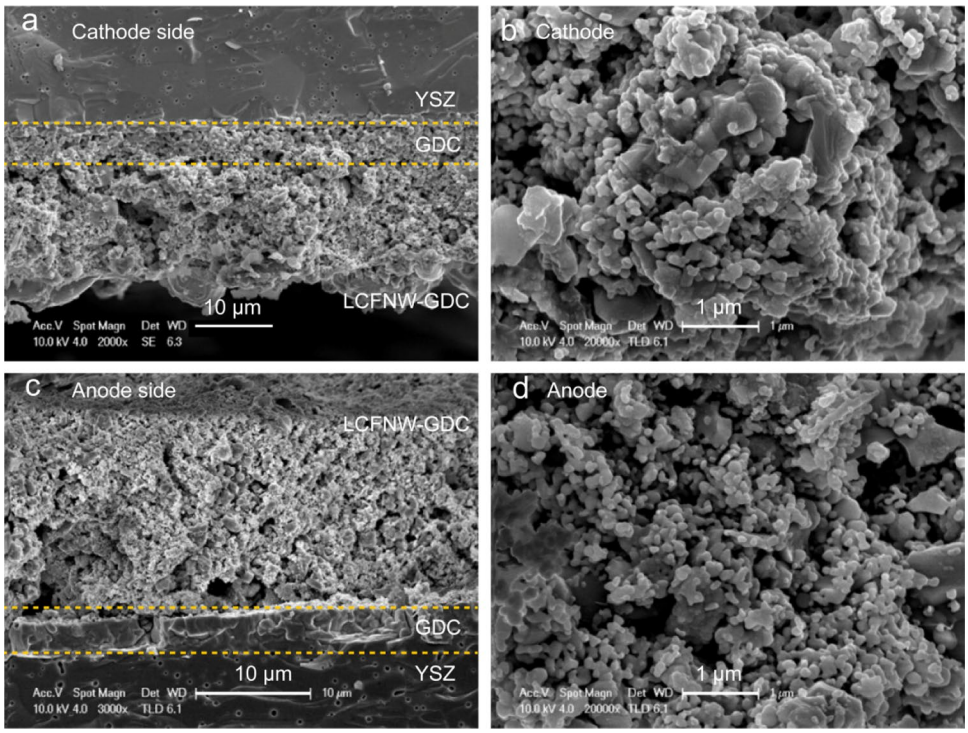

Fig. 8 SEM image of cell morphology after stability test, **a** cathode side, **b** cathode, **c** anode side and **d** anode

electrodes and the GDC barrier is about 20 μm and 5 μm, respectively. The electrodes had porous microstructure and uniform particle size distribution as shown in Fig. 8b, d, which provides more electrocatalytic active sites for the electrochemical reaction. The nanoparticles can be found on the surface of the cathode side after reduction, which is beneficial to the electrocatalytic activity of the electrode.

4 Conclusion

In this work, the LCFNW electrode powder was synthesized by the sol–gel method, and the LCFNW-GDC|GDC|YSZ|GDC|LCFNW-GDC symmetric cell was prepared and showed good electrochemical performance both in SOFCs and SOECs modes. The LCFNW can maintain a stable perovskite structure both in air and hydrogen atmosphere. In SOFCs mode, the symmetric cell based on LCFNW-GDC composite electrode can achieve a maximum power density of 0.38 $W{\cdot}cm^{-2}$ and a R_p of 0.24 $\Omega{\cdot}cm^2$ at 800 °C. In SOECs mode, the maximum current density of the symmetric cell for pure CO_2 electrolysis at 800 °C can reach 1.34 $A{\cdot}cm^{-2}$. Both R_s and R_p decrease with increasing applied voltage and temperature. In addition, the cell shows good stability in both SOFCs and SOECs modes, and the cell microstructure also remains decent after the stability test. The results show that LCFNW has good electrocatalytic activity and stability, which confirms that doping tungsten

is indeed beneficial to improve the electrocatalytic activity of perovskite oxide. Tungsten doping strategy can also be extended to other electrocatalytic fields such as metal-air batteries, ammonia synthesis, etc.

Acknowledgements We gratefully appreciate for financial support from National Key R&D Program for Young Scientists (2021YFA1501900), National Natural Science Foundation of China (52272257), Material Science and Engineering Discipline Guidance Fund of China University of Mining and Technology (CUMTMS202203), Foundation of State Key Laboratory of Clean and Efficient Coal Utilization, Taiyuan University of Technology (Grant No. SKL2022008), the Jiangsu Provincial Shuangchuang Doctor Program (JSSCBS20211224), Young Elite Scientists Sponsorship Program by (CAST2022QNRC001) and the Open Sharing Fund for the Large-scale Instruments (DYGX-2021-026) and Equipments of China University of Mining and Technology (CUMT) Analytical for sample characterizations assistance.

Author contributions XJ: conceptualization, investigation, writing—original draft. AG: investigation, validation. YX: formal analysis, investigation. XW: funding acquisition, investigation. FJ: methodology, investigation. YL: investigation, data curation. YT: supervision, data curation, review and editing.

Data availability The raw/processed data can be provided on the reasonable request.

Declarations

Conflict of interest The authors state that there are no conflict of interest.

References

1. Xu Q, Guo Z, Xia L, He Q, Li Z, Bello IT, Zheng K, Ni M. A comprehensive review of solid oxide fuel cells operating on various promising alternative fuels. Energy Convers Manag. 2022;253:115175.
2. Ndubuisi A, Abouali S, Singh K, Thangadurai V. Recent advances, practical challenges, and perspectives of intermediate temperature solid oxide fuel cell cathodes. J Mater Chem A. 2022;10(5):2196.
3. Shimada H, Yamaguchi T, Kishimoto H, Sumi H, Yamaguchi Y, Nomura K, Fujishiro Y. Nanocomposite electrodes for high current density over 3 $A{\cdot}cm^{-2}$ in solid oxide electrolysis cells. Nat Commun. 2019;10:1.
4. Song Y, Zhang X, Xie K, Wang G, Bao X. High-temperature CO_2 electrolysis in solid oxide electrolysis cells: developments, challenges, and prospects. Adv Mater. 2019;31(50):1902033.
5. Bian L, Duan C, Wang L, Chen Z, Hou Y, Peng J, Song X, An S, O'Hayre R. An all-oxide electrolysis cells for syngas production with tunable H_2/CO yield via co-electrolysis of H_2O and CO_2. J Power Sources. 2021;482:228887.
6. Qiu P, Sun S, Yang X, Chen F, Xiong C, Jia L, Li J. A review on anode on-cell catalyst reforming layer for direct methane solid oxide fuel cells. Int J Hydrogen Energy. 2021;46(49):25208.
7. Pan J, Ye Y, Zhou M, Sun X, Ling Y, Yashiro K, Chen Y. Improving the activity and stability of Ni-based electrodes for solid oxide cells through surface engineering: recent progress and future perspectives. Mater Rep Energy. 2021;1(2):100025.
8. Mosiałek M, Zimowska M, Kharytonau D, Komenda A, Górski M, Krzan M. Improvement of $La_{0.8}Sr_{0.2}MnO_{3-\delta}$ cathode material for solid oxide fuel cells by addition of $YFe_{0.5}Co_{0.5}O_3$. Materials. 2022;15(2):642.
9. Zhuang Z, Li Y, Yu R, Xia L, Yang J, Lang Z, Zhu J, Huang J, Wang J, Wang Y. Reversely trapping atoms from a perovskite surface for high-performance and durable fuel cell cathodes. Nat Catal. 2022;5:300.
10. Zhu K, Luo B, Liu Z, Wen X. Recent advances and prospects of symmetrical solid oxide fuel cells. Ceram Int. 2022;48(7):8972.
11. Tian Y, Abhishek N, Yang C, Yang R, Choi S, Chi B, Pu J, Ling Y, Irvine JT, Kim G. Progress and potential for symmetrical solid oxide electrolysis cells. Matter. 2022;5(2):482.
12. Tian Y, Zheng H, Zhang L, Chi B, Pu J, Li J. Direct electrolysis of CO_2 in symmetrical solid oxide electrolysis cell based on $La_{0.6}Sr_{0.4}Fe_{0.8}Ni_{0.2}O_{3-\delta}$ electrode. J Electrochem Soc. 2018;165:F17.
13. Badding ME, Brown JL, Ketcham TD, Julien DJS. Solid oxide fuel cells with symmetric composite electrodes. US Patents: US6630267B2; 2003.
14. Fan W, Sun Z, Wang J, Zhou J, Wu K, Cheng Y. A new family of Ce-doped $SmFeO_3$ perovskite for application in symmetrical solid oxide fuel cells. J Power Sources. 2016;312:223.
15. Ma Z, Sun C, Ma C, Wu H, Zhan Z, Chen L. Ni doped $La_{0.6}Sr_{0.4}FeO_{3-\delta}$ symmetrical electrode for solid oxide fuel cells. Chin J Catal. 2016;37(8):1347.
16. Rath MK, Kossenko A, Zinigrad M, Kalashnikov A. In-operando gas switching to suppress the degradation of symmetrical solid oxide fuel cells. J Power Sources. 2020;476:228630.
17. Li B, He S, Li J, Yue X, Irvine JT, Xie D, Ni J, Ni C. A Ce/Ru codoped $SrFeO_{3-\delta}$ perovskite for a coke-resistant anode of a symmetrical solid oxide fuel cell. ACS Catal. 2020;10:14398.
18. Petric A, Huang P, Tietz F. Evaluation of La–Sr–Co–Fe–O perovskites for solid oxide fuel cells and gas separation membranes. Solid State Ionics. 2000;135(1–4):719.
19. Zhang Y, Nicholas JD. Evidence that surface-segregated Sr phases can be removed in LSCF via ceria pre-infiltration, are less apt to form in SSC. J Electrochem Soc. 2021;168:024522.
20. Kumar RV, Khandale A. A review on recent progress and selection of cobalt-based cathode materials for low temperature-solid oxide fuel cells. Renew Sustain Energy Rev. 2022;156:111985.
21. Wang W, Tian Y, Liu Y, Abhishek N, Li Y, Chi B, Pu J. Tailored Sr–Co-free perovskite oxide as an air electrode for high-performance reversible solid oxide cells. Sci China Mater. 2021;64:1621.
22. Tian Y, Liu Y, Jia L, Naden A, Chen J, Chi B, Pu J, Irvine JT, Li J. A novel electrode with multifunction and regeneration for highly efficient and stable symmetrical solid oxide cell. J Power Sources. 2020;475:228620.
23. Su T, Zhang T, Xie H, Zhong J, Xia C. Investigation into structure and property of W and Ti co-doped $SrFeO_3$ perovskite as electrode of symmetrical solid oxide fuel cell. Int J Hydrog Energy. 2022;47(36):16272.
24. Song J, Zhu T, Chen X, Ni W, Zhong Q. Cobalt and titanium substituted $SrFeO_3$ based perovskite as efficient symmetrical electrode for solid oxide fuel cell. J Mater. 2020;6(2):377.
25. Gou M, Ren R, Sun W, Xu C, Meng X, Wang Z, Qiao J, Sun K. Nb-doped $Sr_2Fe_{1.5}Mo_{0.5}O_{6-\delta}$ electrode with enhanced stability and electrochemical performance for symmetrical solid oxide fuel cells. Ceram Int. 2019;45(12):15696
26. Arrive C, Delahaye T, Joubert O, Gauthier GH. Study of (La, Sr)(Ti, Ni)$O_{3-\delta}$ materials for symmetrical Solid oxide cell electrode—part a: synthesis and structure analysis in air. Ceram Int. 2019;45(14):17969.
27. Tian Y, Yang C, Li Y, He S, Wang X, Ling Y, Li W, Chi B, Pu J. A Simple Sc doping strategy to enhance electrocatalytic activity and stability in symmetrical solid oxide cells. J Electrochem Soc. 2021;168:104515.
28. Tian Y, Wang W, Liu Y, Zhang L, Jia L, Yang J, Chi B, Pu J, Li J. Cobalt-free perovskite oxide $La_{0.6}Sr_{0.4}Fe_{0.8}Ni_{0.2}O_{3-\delta}$ as active

and robust oxygen electrode for reversible solid oxide cells. ACS Appl Energy Mater. 2019;2(5):3297.
29. Shi H, Su C, Ran R, Cao J, Shao Z. Electrolyte materials for intermediate-temperature solid oxide fuel cells. Prog Nat Sci Mater Int. 2020;30(6):764.
30. Wang F, Zhou Q, He T, Li G, Ding H. Novel $SrCo_{1-y}Nb_yO_{3-\delta}$ cathodes for intermediate-temperature solid oxide fuel cells. J Power Sources. 2010;195(12):3772.
31. Du Z, Zhao H, Shen Y, Wang L, Fang M, Świerczek K, Zheng K. Evaluation of $La_{0.3}Sr_{0.7}Ti_{1-x}Co_xO_3$ as a potential cathode material for solid oxide fuel cells. J Mater Chem A. 2014;2(26):10290.
32. Wei B, Lü Z, Li S, Liu Y, Liu K, Su W. Thermal and electrical properties of new cathode material $Ba_{0.5}Sr_{0.5}Co_{0.8}Fe_{0.2}O_{3-\delta}$ for solid oxide fuel cells. Electrochem Solid State Lett. 2005;8:A428.
33. Gu Y, Zhang Y, Ge L, Zheng Y, Chen H, Guo L. YSZ electrolyte support with novel symmetric structure by phase inversion process for solid oxide fuel cells. Energy Convers Manag. 2018;177:11.
34. Bastidas DM, Tao S, Irvine JT. A symmetrical solid oxide fuel cell demonstrating redox stable perovskite electrodes. J Mater Chem. 2006;16(17):1603.
35. Guo Y, Guo T, Zhou S, Wu Y, Chen H, Ou X, Ling Y. Characterization of $Sr_2Fe_{1.5}Mo_{0.5}O_{6-\delta}$–$Gd_{0.1}Ce_{0.9}O_{1.95}$ symmetrical electrode for reversible solid oxide cells. Ceram Int. 2019;45(8):10969.
36. Tian D, Lin B, Yang Y, Chen Y, Lu X, Wang Z, Liu W, Traversa E. Enhanced performance of symmetrical solid oxide fuel cells using a doped ceria buffer layer. Electrochim Acta. 2016;208:318.
37. Ruiz-Morales JC, Canales-Vazquez J, Pena-Martmez J, Lopez DM, Nunez P. On the simultaneous use of $La_{0.75}Sr_{0.25}Cr_{0.5}Mn_{0.5}O_{3-\delta}$ as both anode and cathode material with improved microstructure in solid oxide fuel cells. Electrochim Acta. 2006;52(1):278.
38. Luo X, Yang Y, Yang Y, Tian D, Lu X, Chen Y, Huang Q, Lin B. Reduced-temperature redox-stable LSM as a novel symmetrical electrode material for SOFCs. Electrochim Acta. 2018;260:121.
39. dos Santos-Gómez L, Porras-Vázquez JM, Losilla ER, Marrero-López D, Slater PR. Investigation of PO_4^{3-} oxyanion-doping on the properties of $CaFe_{0.4}Ti_{0.6}O_{3-\delta}$ for potential application as symmetrical electrodes for SOFCs. J Alloys Compd. 2020;835:155437.
40. Zhang Y, Zhao H, Du Z, Świerczek K, Li Y. High-performance $SmBaMn_2O_{5+\delta}$ electrode for symmetrical solid oxide fuel cell. Chem Mater. 2019;31(10):3784.
41. Cao Z, Wei B, Miao J, Wang Z, Lü Z, Li W, Zhang Y, Huang X, Zhu X, Feng Q. Efficient electrolysis of CO_2 in symmetrical solid oxide electrolysis cell with highly active $La_{0.3}Sr_{0.7}Fe_{0.7}Ti_{0.3}O_3$ electrode material. Electrochem Commun. 2016;69:80.
42. Torrell M, Garcia-Rodriguez S, Morata A, Penelas G, Tarancon A. Co-electrolysis of steam and CO_2 in full-ceramic symmetrical SOECs: a strategy for avoiding the use of hydrogen as a safe gas. Faraday Discuss. 2015;182:241.
43. Peng X, Tian Y, Liu Y, Wang, Jia L, Pu J, Chi B, Li J. An efficient symmetrical solid oxide electrolysis cell with LSFM-based electrodes for direct electrolysis of pure CO_2. J CO_2 Util. 2020;36:18.
44. Li Y, Li Y, Wan Y, Xie Y, Zhu J, Pan H, Zheng X, Xia C. Perovskite oxyfluoride electrode enabling direct electrolyzing carbon dioxide with excellent electrochemical performances. Adv Energy Mater. 2019;9(3):1803156.